Microchemical Journal 170 (2021) 106765

Contents lists available at ScienceDirect

Microchemical Journal

journal homepage: www.elsevier.com/locate/microc

Tergitol@SiO_2@Fe_3O_4 magnetic nano-material and experimental design methodology: An effective and selective adsorbent for solid phase microextraction and flame atomic absorption spectrometric analysis of lead in different matrixes

Nail Altunay [a,*], Adil Elik [a], Gökhan Sarp [b], Erkan Yılmaz [b], Halil İbrahim Ulusoy [c]

[a] Sivas Cumhuriyet University, Faculty of Sciences, Department of Chemistry, TR-58140 Sivas, Turkey
[b] Erciyes University, Faculty of Pharmacy, Department of Analytical Chemistry, TR-58140 Kayseri, Turkey
[c] Sivas Cumhuriyet University, Faculty of Pharmacy, Department of Analytical Chemistry, TR-58140 Sivas, Turkey

ARTICLE INFO

Keywords:
Magnetic nanoparticles
Experimental design
Solid phase microextraction
Lead
Real samples
Flame atomic absorption spectroscopy
Tergitol@SiO_2@Fe_3O_4

ABSTRACT

In current paper, we synthesized a new and functional magnetic Tergitol@SiO_2@Fe_3O_4. The synthesized magnetic nano-material was characterized in detail using transmission electron microscopy, energy dispersive spectrometer, X-ray photoelectron spectroscopy, and fourier transform infrared spectrometer. Then, the applicability of the synthesized nano-material to the separation and preconcentration of Pb(II) ions was investigated prior to flame atomic absorption spectrometric determination. In order to ensure efficient and selective extraction of Pb(II), major variables such as pH, adsorbent amount, and adsorption time were optimized by multivariate methodology based on Box-Behnken design. Under the optimized conditions, linearity, detection limit, enhancement factor, and relative standard deviation (RSD%) were 0.2–250 μg L^{-1}, 0.07 μg L^{-1}, 84, and 1.8%, respectively. Accuracy and precision of the optimized method were investigated by using two certified reference materials (INCT-TL-1-tea leaves and SRM-1643e Trace elements in water), and good recoveries (94.7–103.9%) with low RSDs were achieved. Finally, the optimized method was successfully applied for the determination and separation of lead in different matrixes.

1. Introduction

Unlike organic pollutants, heavy metals are persistent and difficult to biodegrade. These metals can be grouped into three classes, potentially toxic (Hg, Cd, and Pb, etc.), possibly essential (Co, and Ni, etc.) and essential (Fe, Se, and, Zn, etc.) [1,2]. Pb is not found naturally in food products. However, trace levels of Pb can be found in foods as a result of contamination from metallic equipment used during food processing [3]. The Pb is a neurotoxic poison and is reported to affect both the nervous system and the brain [4]. It has been stated that lead also affects the immune system, decreases the resistance against bacteria and viruses and causes an increase in infections, and also increases the risk factors for kidney tumors and cancer risk [5,6]. Due to these negative reasons, it is still important to develop sensitive, cheap and usable new analytical methods for determining the amount of lead in food and environmental samples.

However, determining lead ions with high accuracy and precision at very low concentrations is difficult due to the presence of other ions and organic substances in the sample matrix [7]. Therefore, an efficient sample preparation step must be applied to separate or preconcentrate lead ions from the matrix before analytical measurement. In this context, various sample preparation procedures such as air assisted liquid phase microextraction based on deep eutectic solvent (AA-DES-LPME) [8], ultrasonic assisted-dispersive solid phase extraction based on ion-imprinted polymer (UA-DSPE-IIP) [9], cloud point extraction (CPE) [10], dispersive liquid–liquid microextraction (DLLME) [11], centrifuge-less deep eutectic solvent based magnetic nanofluid-linked air-agitated liquid–liquid microextraction (CL-DES-MNF-AALLME) [12], deep eutectic solvent-based liquid phase microextraction (DES-LPME) [13], ultrasound-assisted surfactant-enhanced emulsification microextraction (UASEME) [14], ultrasound-assisted magnetic retrieval-linked ionic liquid dispersive liquid–liquid microextraction

* Corresponding author.
E-mail address: naltunay@cumhuriyet.edu.tr (N. Altunay).

https://doi.org/10.1016/j.microc.2021.106765
Received 12 May 2021; Received in revised form 12 August 2021; Accepted 14 August 2021
Available online 25 August 2021

(UA-MR-IL-DLLME) [15], green solvent-based ultrasonic assisted dispersive liquid–liquid microextraction (GS-UADLLME) [16] and magnetic cobalt particles based dispersive solid-phase microextraction (Co-MP-DSPME) [17] have been reported for the separation and preconcentration of lead from different sample matrices. Magnetic solid phase (MSPE) approaches was attracted attention in the last decades owing to easy applicable properties. A known, the most important problem in conventional SPE approaches is separating of solid and aqua phases [18,19]. Filtration, centrifugation, and flotation techniques are generally used for effectively phase separation. Almost, none of these methods can separate phases completely. In MSPE methods, solid sorbents can be easily separated by using anexternal magnets. Magnetic properties of solid phases helps their simple and fast separation. There are an of applications about use of magnetic particles in trace analysis of inorganic and organic species [20,21].

After sample preparation, spectroscopic techniques such as electrothermal atomic absorption spectrometry (ETAAS) [22], flame atomic absorption spectrometry (FAAS) [23], inductively coupled plasma optical emission spectrometry (ICP-OES) [24] atomic fluorescence spectrometry (AFS) [25], inductively coupled plasma-mass spectrometry (ICP-MS) [26], resolution continuum source graphite furnace atomic absorption spectrometry (RCS-GFAAS) [27] and inductively coupled plasma-atomic emission spectroscopy (ICP-AES) [28] were frequently reported for the determination of lead in in waters, foods, beverages and biological samples. ICP-MS, ICP-AES and ICP-OES techniques were preferred by scientists due to the advantage of multi-element determination at trace levels. However, these techniques were relatively expensive and the daily operating and maintenance costs were also high [29]. But, the FAAS offers low cost, rapid measurement, cheapness, and simple operation [29].

Experimental modelling for optimization studies allows predicting relationships between experimental factors through a regression function [30]. Experimental modelling is preferred to rigorously evaluate all variable types of an analytical method, rather than the general practice of “changing one variable at a time” because it is economical, time-saving, and requires less experimentation [31]. Moreover, the statistical significance of the factors investigated can be determined using the developed mathematical design and optimum conditions can be obtained from this design to find the most appropriate analytical factor.

In the scope of this study, a new magnetic nanoparticle was synthetized and characterized for sensitive analysis of lead ions in real samples. New material, Tergitol@SiO_2@Fe_3O_4, was used the first times for this study and optimization of the proposed MSPE approaches was successively performed step by step.

2. Experimental

2.1. Reagents and solutions

A Stock solution (1000 μg mL^{-1}) of Pb(II) ions was prepared by dissolving $Pb(NO_3)_2$ $3H_2O$ salt (Sigma-Aldrich, St. Louis, MO, USA) in water, and was stored in a refrigerator at 4 °C. Standard working solutions were freshly prepared by sequential dilution of the stock solution. Iron (II) chloride, iron (III) chloride, tetraethyl orto silicate (TEOS), and Tergitol were purchased from Sigma, Aldrich. Ethanol (99.8%, d = 0.789 g mL^{-1}, Sigma), methanol (99.8%, d = 0.792 g mL^{-1}, Merck), ethanol in nitric acid, methanol in nitric acid, tetrahydrofuran (99.8%, d = 0.89 g cm^{-3}, THF, Merck), and acetone (99.8%, d = 0.79 g cm^{-3}, Merck) were tested as the desorption solvent. pH solutions (in the range of 2.5–9) were prepared using phthalate, borate, citrate and phosphate buffer solutions. Before solid-phase microextraction studies, all materials were thoroughly cleaned by soaking in 1.0 mol L^{-1} HNO_3 solution, and then rinsed with water. To test the reliability of the obtained analytical results, two certified reference materials (CRMs) such as INCT-TL-1-tea leaves and SRM-1643e Trace elements in water were analyzed with the optimized method.

2.2. Equipment

Analytical signal was measured using a Shimadzu AAS-6300 model (Kyoto, Japan) flame atomic absorption spectrometry (FAAS) equipped with lead hollow cathode lamp. Measurement parameters including wavelength, lamp current, spectral bandwidth, burner height and acetylene and air flow rates were 217 nm, 10 mA, 0.5 nm, 5 mm, and 1.8/17 L min^{-1}, respectively. Multi Bio RS-24 model orbital rotator (BioSan, ProfiLab24 GmbH, Landsberger Berlin, Germany) was employed in the adsorption step. A pH-meter combined with glass electrode (Selecta 2001 Sartorius, North America) was used to adjust the pH of the solutions. A neodymium magnet was used to accelerate the separation of the solid adsorbent from the aqueous phase. The - vortex VG3 model (IKA GmbH, Germany) was utilized for desorption - step. The characterization of the adsorbent was evaluated by Fourier transform infrared spectroscopy (PerkinElmer Lambda 25), scanning electron microscopy (Zeiss Gemini 500) and energy-dispersive X-ray spectroscopy (Zeiss Gemini 500) techniques.

2.3. Sample collection

To investigate the feasibility of the present study, tap water, bottled water, river water, and well-water were collected from our laboratory, local market in Sivas (Turkey), the coastal area of Kızılırmak river passing through Sivas, and agricultural land in Sivas, respectively. All water samples were filtered through membrane filters (Millipore, 0.22 μm) and stored in polyethylene bottles prior to solid-phase microextraction.

As another application of the proposed method, meat doner, chicken doner, meatballs, grilled chicken and fish were used by considering optimization procedure. Each sample was analyzed in 3 repetitions. Samples were taken between March and June 2017 from different restaurants in Sivas, Turkey and stored in the freezer –20℃ [32].

2.4. Sample preparation

Microwave digestion system was used for preparation of meat samples. PTFE vessels were cleaned using 10 mL of concentrated HNO_3, heated for 15 min at 180 °C (800 W), and then rinsed with ultrapure water heated for 15 min at 180 °C before each digestion. All samples were accurately weighted as 0.50 g, transferred directly into microwave vessels, and added 5 mL of concentrated HNO_3. The digestion program was chosen in agreement with manufacturer’s recommendations [33].

2.5. Synthesis of magnetic adsorbent

Tergitol@SiO_2@Fe_3O_4 magnetic nanoparticles were produced by using solve thermal synthesis method in the medium of inert nitrogene. For this purpose, 3 mmol of iron (III) chloride and 2 mmol of iron (II) chloride were dissolved in a solution containing 50 mL of 0.001 M HCl solution. Then, 50 mL of 50 % methyl alcohol was added to this solution. After, clear solution was obtained, 20 mL of ammonia solution was added to this solution drop by drop. Fe_3O_4 particles was obtained with black-brown color end of this process. Particles was separated by external magnet and dried at 40 °C. In the second step, 2.0 g of Fe_3O_4 particles were dispersed in 50 mL of 50 % methanol by an ultrasonication. Following adding of 1 mL ammonia, 3 mL Tergitol was added solution while it was vigorously mixing at 500 rpm on a magnetic stirrer in the presence of inert atmosphere of nitrogen. The resulting mixture was allowed to react in the reactor at 60 °C for 12 h. Tergitol@SiO_2@-Fe_3O_4, magnetic nanoparticles obtained after the completion of reaction process were collected with an external neodymium magnet, then washed several times with deionized water and ethanol and dried in a vacuum oven.

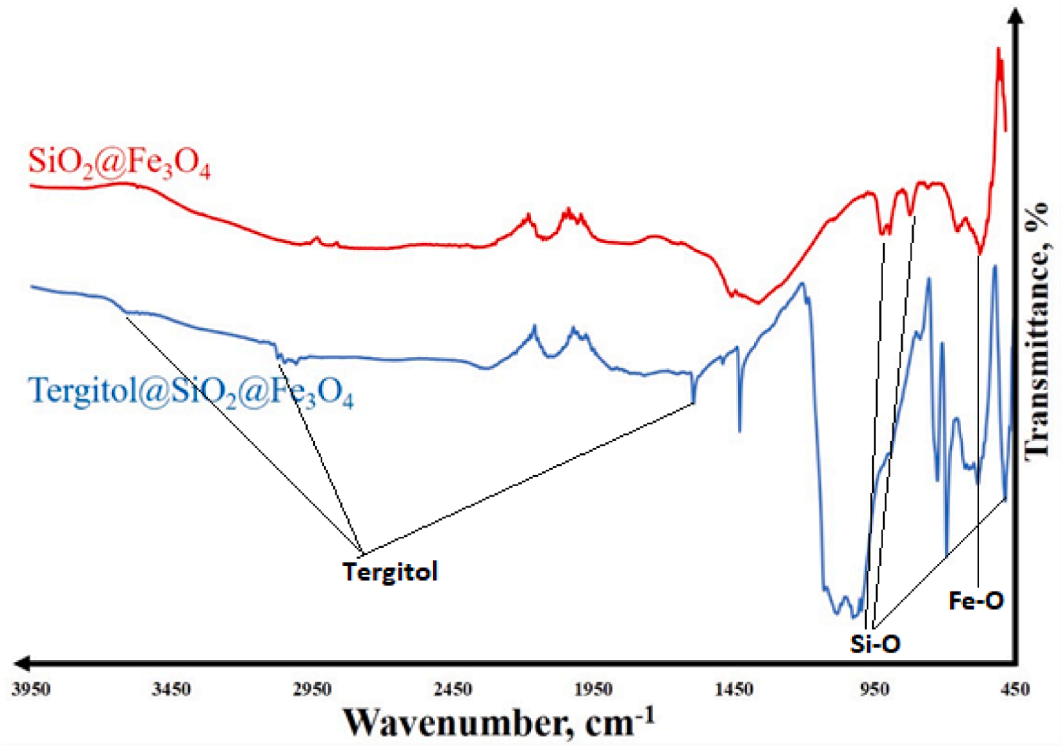

a

Fig. 1a. FT-IR spectrum of $SiO_2@Fe_3O_4$ (A) and Tergitol@$SiO_2@Fe_3O_4$ (B) nanomaterials.

2.6. Box–Behnken design

Generally, the application of experimental design (DoE) reduces the number of experiments in optimization studies and provides less uncertain extraction conditions, thus facilitating data interpretation [31]. Therefore, the levels of important experimental variables affecting the separation and preconcentration of Pb (II) ions and the interaction effects between them were optimized by the Box–Behnken design (BBD).

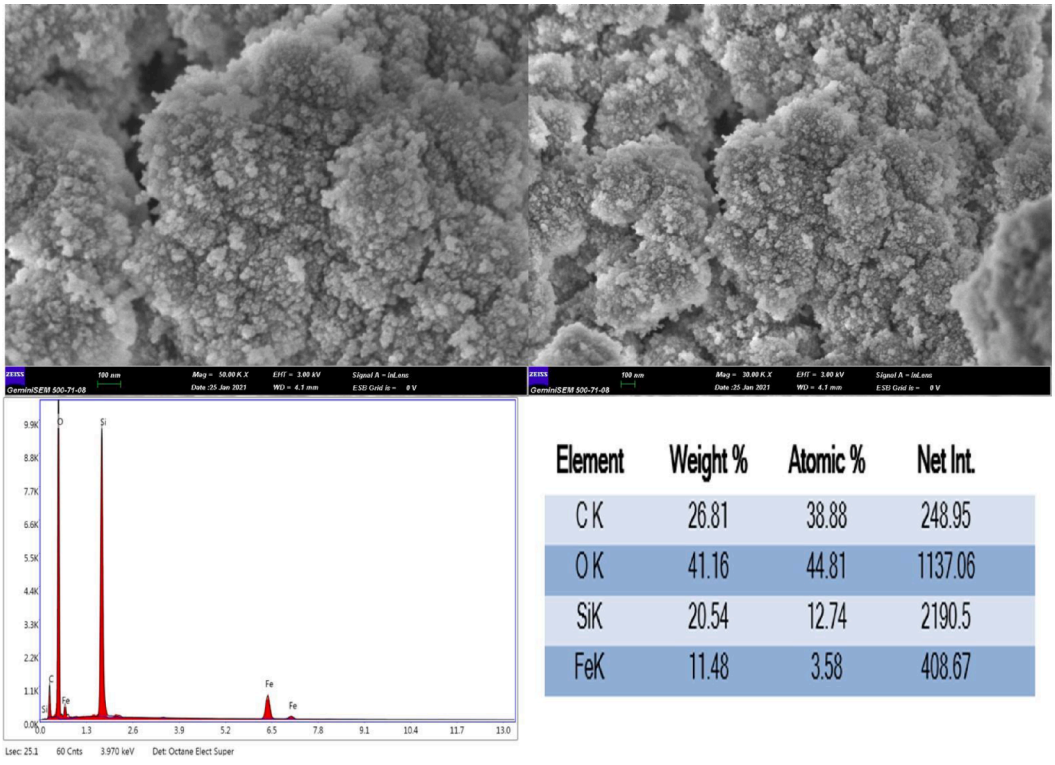

Element	Weight %	Atomic %	Net Int.
C K	26.81	38.88	248.95
O K	41.16	44.81	1137.06
SiK	20.54	12.74	2190.5
FeK	11.48	3.58	408.67

Fig. 1b. SEM images and EDX analysis of Tergitol@$SiO_2@Fe_3O_4$ nanomaterial.

Table 1
Analysis of variance (ANOVA) table obtained after applying the BBD design for the full quadratic model.

Source	Sum of Squares	df[a]	Mean Square	F_{value}[b]	p_{value}[c,d]	prob > F
Model	4262.08	9	473.56	2864.66	< 0.0001	significant
X_1	1987.65	1	1987.65	12023.60	< 0.0001	
X_2	181.45	1	181.45	1097.63	< 0.0001	
X_3	72.00	1	72.00	435.54	< 0.0001	
X_1X_2	13.69	1	13.69	82.81	< 0.0001	
X_1X_3	1.56	1	1.56	9.45	0.0152	
X_2X_3	162.56	1	162.56	983.36	< 0.0001	
X_1^2	185.78	1	185.78	1123.84	< 0.0001	
X_2^2	10.82	1	10.82	65.48	< 0.0001	
X_3^2	1745.45	1	1745.45	10558.52	< 0.0001	
Residual	1.32	8	0.1653			
Lack of Fit	0.2075	3	0.0692	0.3102	0.8179	not significant
Pure Error	1.11	5	0.2230			
Cor Total	4263.40	17				
Std. Dev.	0.407		R^2	0.999		
Mean	68.14		Adjusted R^2	0.988		
C.V. %	0.597		Predicted R^2	0.968		

[a]Degrees of freedom.
[b]Test for comparing model variance with residual (error) variance.
[c]Probability of seeing the observed F value if the null hypothesis is true.

The main advantage of the BBD is that it does not include variations where all experimental variables are at their highest or lowest levels at the same time. Therefore, this design is useful for avoiding experimental studies performed under extreme conditions. In this context, a 3-variable and 3-level BBD design was established. Details of the current design were given in Supplementary Material Table S1.

2.7. Optimized magnetic-SPME procedure

First, a 30 mL of sample solution containing 60 μg of Pb(II) was poured into a 50 mL-conical centrifuge tube, and adjusted to pH 4.7 using a phthalate buffer solution. Second, 41.5 mg of synthesized magnetic nanoparticles (Tergitol@SiO_2@Fe_3O_4) were carefully weighed and added to the sample solution. Third, the tube was placed in an orbital shaker and shaken at 100 rpm for 11.5 min to accelerate the adsorption of Pb(II) ions in the sample solution to the magnetic-

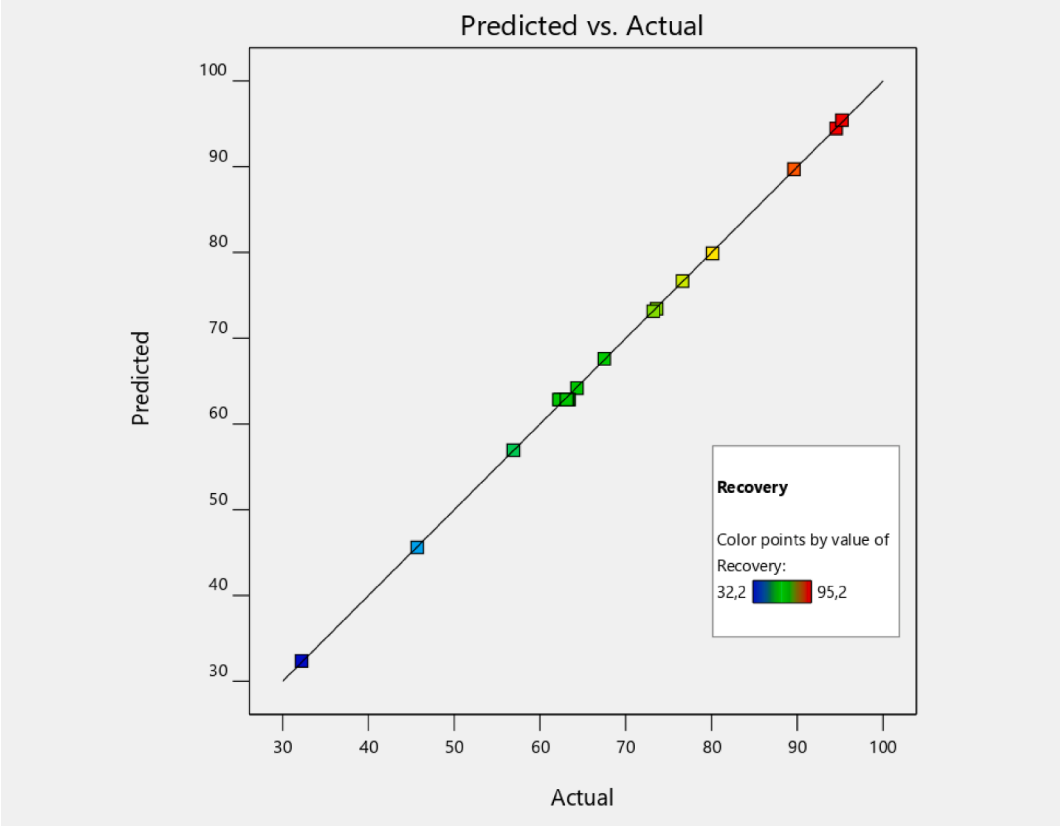

(a)

Fig. 2a. Correlation of experimental and predicted values.

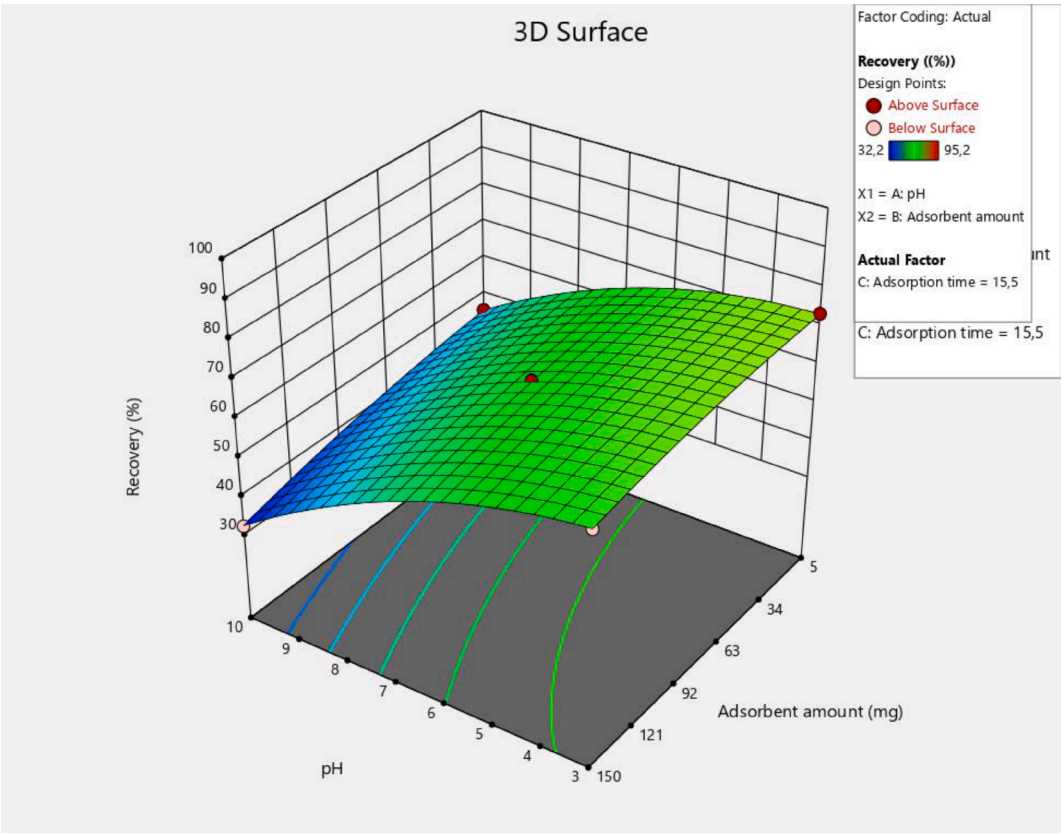

(b)

Fig. 2b. 3D surface plot of pH-adsorbent amount for recovery of Pb(II) ions.

Tergitol@SiO_2@Fe_3O_4. fourth, a neodymium magnet was placed at the bottom of the tube to separate the Tergitol@SiO_2@Fe_3O_4 magnetic nanoparticles from the aqueous phase and the supernatant was decanted. Fifth, the desorption of Pb (II) ions adsorbed on the solid was achieved by adding 1.5 mL of acidic ethanol and then vortexing for 1 min. Finally, the eluent solution was aspirated to the FAAS for absorbance measurements of lead. The amount of lead in the selected samples was calculated with the help of the obtained calibration equation. All studies were also carried out with the sample blank.

3. Results and discussion

3.1. Characterization studies

The characterization of the Tergitol@SiO_2@Fe_3O_4 nanomaterial was evaluated by Fourier transform infrared spectroscopy, scanning electron microscopy and energy-dispersive X-ray spectroscopy techniques. The FTIR spectra of pristine SiO_2@Fe_3O_4 and Tergitol@SiO_2@Fe_3O_4 nanomaterials are shown in Fig. 1a. A characteristic peak at around 544 cm^{-1} belongs to Fe–O bond vibration of Fe_3O_4 nanoparticles. The characteristic bands at 1083, 863 and 451 cm^{-1} are assigned for asymmetric, symmetric and bending vibrations of Si–O bonds, respectively. The peaks around at 3586, 3000, 1592 and 1079 cm^{-1} are assigned for O–H, C–H, C = C and C-O streching vibrations of Tergitol, respectively. Morphological characterization of the Tergitol@SiO_2@-Fe_3O_4 nanomaterial was carried out by SEM analysis (Fig. 1b). The images obtained showed that particle size of the SiO_2 and Fe_3O_4 particles are lower than 100 nm and distribution of particles are homogeneous. EDX analysis showed that Tergitol@SiO_2@Fe_3O_4 nanomaterial was successfully synthesized.

3.2. BBD results

To find the best adsorption conditions of Pb (II) ions, major variables such as pH, adsorbent amount, and adsorption time were optimized by BBD design. The BBD based on 18 experimental studies consisting of the center, factorial and axial points were used for the optimization of the relevant variables. Supplementary Material Table S1 shows the matrix of independent variables and their corresponding experimental and predicted recovery for Pb(II) ions.

3.2.1. ANOVA analysis

ANOVA analysis (see Table 1) was performed using the analytical data obtained as a result of applying the experimental modeling in Supplementary Material Table S1. ANOVA analysis provides important analytical data such as meaningful and meaningless interactions in the model, the predictive power of the model, and the reliability of the results. The main factors and their interactions with a probability (P-value) of<0.05 were significant at 95% confidence level. In ANOVA analysis, adsorption variables with a large F value and a small p-value ($p < 0.05$) make a significant contribution to the established model. When Table 1(b) is examined, it can be said that the F-value and p-value of the model are 2864.66 and < 0.0001, respectively, and these values are statistically significant. Also, the p-values of linear, quadratic and square interactions in the experimental model established were lower than 0.05, indicating that all interactions are significant. In addition, the Lack of Fit F-value of 0.31 implies the Lack of Fit is not significant relative to the pure error. There is an 81.79% chance that a Lack of Fit F-value this large could occur due to noise. R^2 value (Predicted) and R^2 (adjusted) value were used to express the quality of fit of the quadratic equation. R^2 (adjusted) value and R^2 (predicted) values were 0.988 and 0.968 respectively. These results confirm that support presence of high

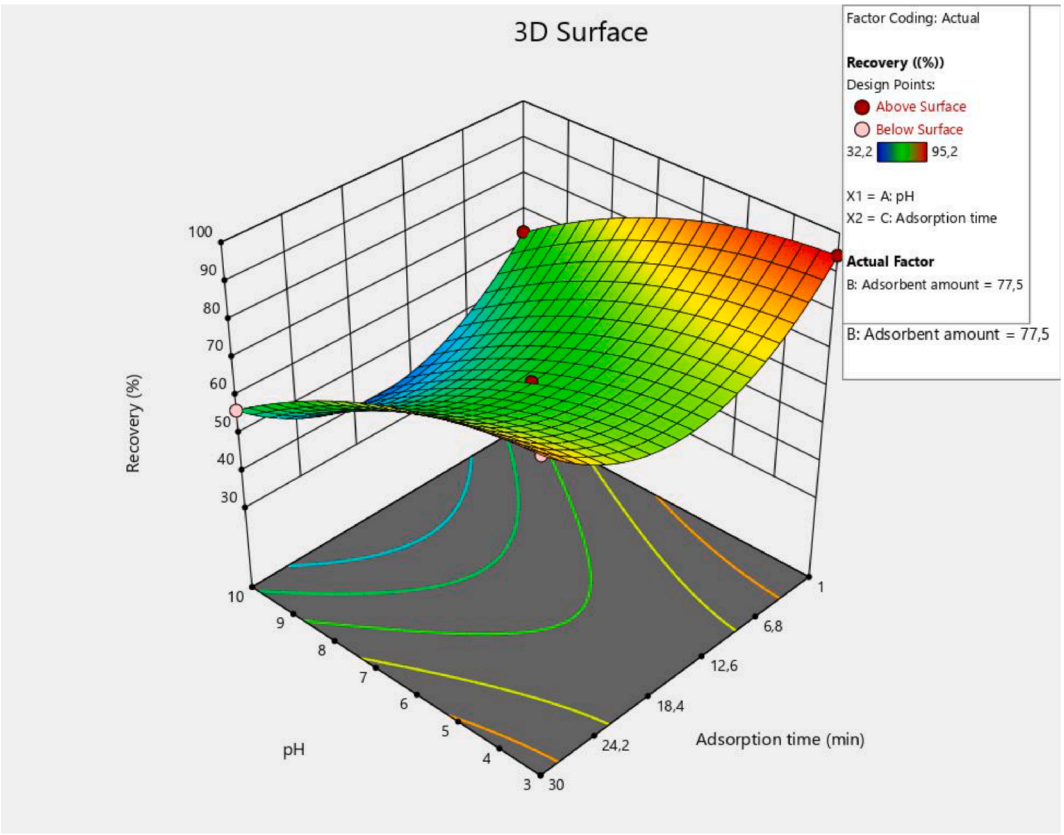

(c)

Fig. 2c. 3D surface plot of pH-adsorption time for recovery of Pb(II) ions.

agreement and correlation between experimental and predicted results. Moreover, the predictive power of the model is 96.8%. As a result, the quadratic model defined the recovery of Pb(II) with the following equation:

$$Recovery\ (\%) = 62{,}85 - 15{,}76X_1 - 4{,}76X_2 - 3{,}00X_3 - 1{,}85X_1X_2 - 0{,}6250X_1X_3 + 6{,}38X_2X_3 - 6{,}52X_1^2 - 1{,}57X_2^2 + 20{,}00X_3^2$$

The values obtained from experimental studies were very close to the predicted values and these results (see Fig. 2a) show that the established model was robust and correct.

3.2.2. Response surface plots

The 3D response surface plots for Pb(II) were demonstrated in Figs. 2 (b–d). These plots were useful to evaluate the interaction between the adsorption variables and determine the optimum value of each variable. These types of plots show the effect of two variables on the recovery at the central point of other variable. Fig. 2(b) illustrate the estimated response surfaces for pH and adsorbent amount. In this Figure, it states that as the pH rises from 3 to 5, the recovery of lead increases and then decreases partially with the continuous increase in pH. For this reason, pH should be chosen lower than 5.0 in optimization studies in order to ensure maximum recovery of Pb(II) ions and effective adsorption on the synthesized magnetic material. The adsorption time was an important variable for Pb (II) ions in the sample solution to hold onto the synthesized magnetic adsorbent. Insufficient adsorption time prevents effective adsorption of Pb(II) ions. Fig. 2(c) illustrate the estimated response surfaces for pH against adsorption time. As can be seen from the corresponding figure, recovery of Pb(II)ions has increased depending on the increase in the adsorption time. The maximum recovery was obtained below pH 5 in an adsorption time of about 15 min. The amount of adsorbent in the sample solution should ensure quantitative recovery of Pb(II) ions and effective phase separation. If the adsorption amount is insufficient, the quantitative adsorption of Pb(II) ions does not occur, consequently, the recovery decreases. Fig. 1(d) illustrate the estimated response surfaces as a function of adsorption time and adsorbent amount. As can be seen from the results, high recoveries were obtained when the adsorption time was less than 15 min and the amount of adsorbent in the range 10–55 mg.

3.2.3. Optimum conditions

Optimization of the adsorption variables to maximize the recovery of the Pb(II) ions via the synthesized HM3 magnetic nano-material was evaluated using the quadratic model within the investigated range of various experimental variables. After generating the polynomial equations, the desirability function in STATISTICA software was used to find the best optimum levels for the adsorption variables in the recovery of Pb(II) ions. The experimental modeling was suggested the optimum values of adsorption variables (viz. pH 4.7, 41.5 mg adsorbent amount, and 11.5 min adsorption time) to achieve the maximum recovery of the Pb(II) ions. The experimental value (96.0 ± 2.2) found as a result of 3 repetitive studies was quite compatible with the predicted value (95.2 ± 3.6) of the model.

3.3. Desorption process

In SPME studies, achieving high extraction efficiency for the selected analyte depends on the type of desorption solvent to be chosen. After separation of the magnetic solid phase from the aqueous solution, the effects of desorption solvents such as ethanol, methanol, acetone, ethanol in nitric acid, methanol in nitric acid, THF, and water on the recovery of Pb(II) ions were examined in equal volume under 1 min

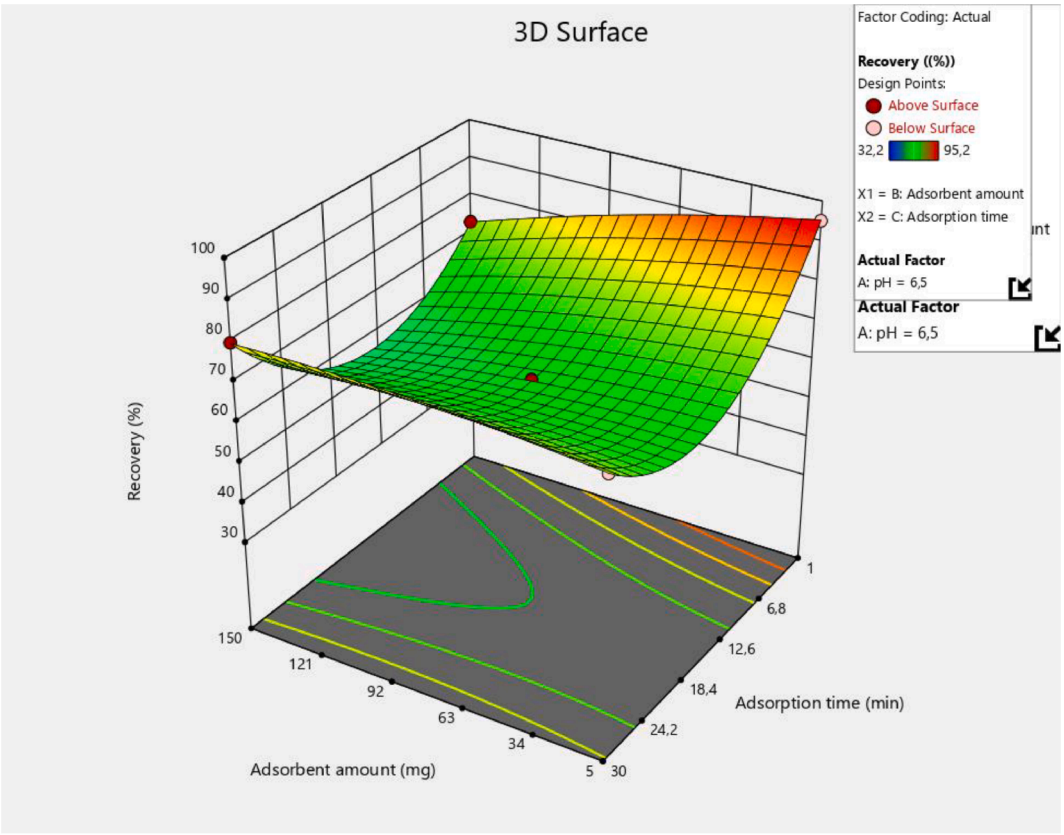

(d)

Fig. 2d. 3D surface plot of adsorption time-adsorbent amount for recovery of Pb(II) ions.

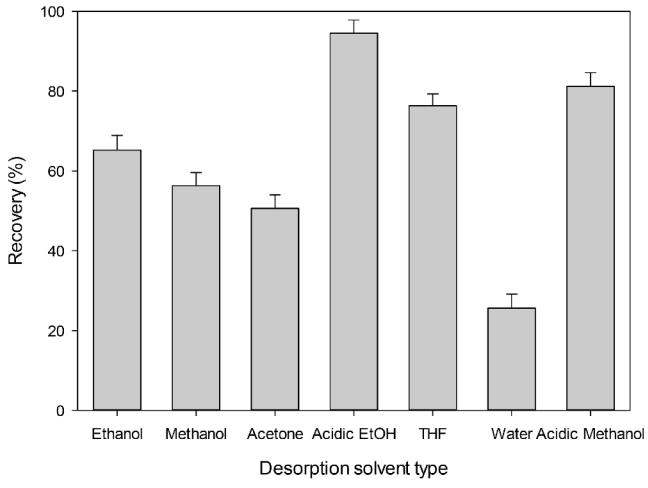

(a)

Fig. 3a. Effect of desorption solvent type on reocvery of Pb(II) ions.

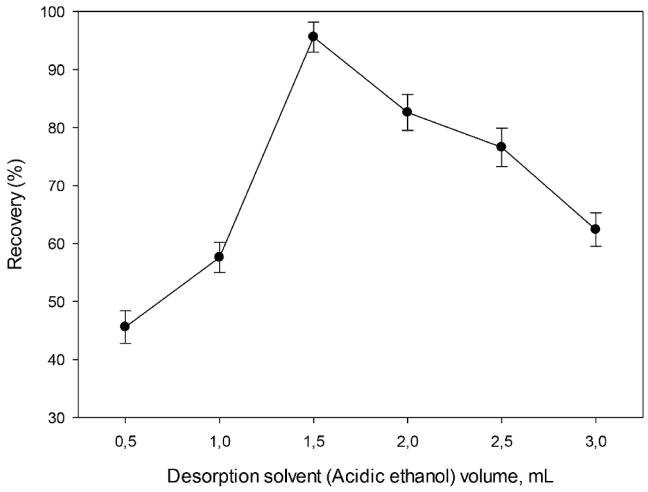

(b)

Fig. 3b. Effect of volume of desorption solvent (acidic ethanol) on recovery of Pb(II) ions.

vortexing. From the results in Fig. 3(a), it is seen that the best recovery is obtained when using acidic ethanol. Once the desorption solvent was chosen as acidic ethanol, the effect of its volume on recovery was tested in the 0.5–3 mL volume range. As result of these studies (see Fig. 3b), quantitative recovery could not be achieved when the volume of acidic ethanol was lower than 1.5 mL, which may be due to the acidic ethanol volume being insufficient for the desorption of lead ions adsorbed on the solid adsorbent. In addition, recovery was decreased due to the increase in acidic ethanol volume, which may be attributed to the dilution of the measuring volume. The effect of vortex time on the recovery of Pb(II) ions was investigated at various times from 0.5 to 5 min. As the vortex time increased from 0.5 to 1 min, the recovery of Pb(II) ions has reached a maximum. According to the obtained results and in order to desorption of Pb(II) ions from the surface of the magnetic adsorbent, vortex time was adjusted at 1 min using 1.5 mL of acidic ethanol as desorption

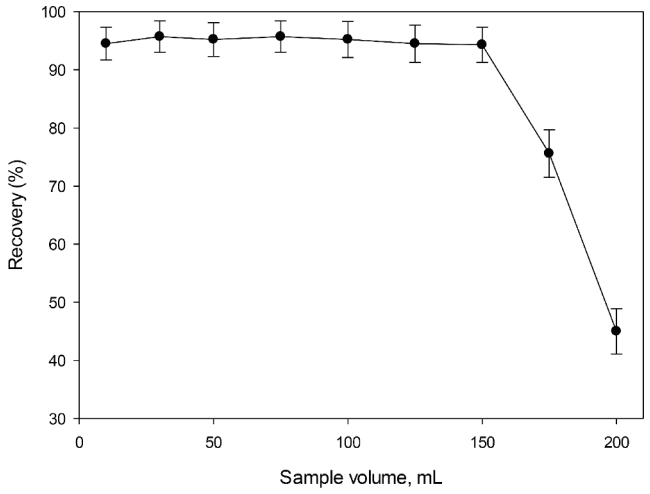

(c)

Fig. 3c. Effect of sample volume on recovery of Pb(II) ions.

solvent.

3.4. Reusability

The cost of the magnetic-SPME procedure is highly dependent on the number of times the solid adsorbent synthesized is used. This is undesirable from a cost perspective, if the efficiency and selectivity of the adsorbent synthesized for the analyte decrease with a small number of uses. Therefore, the reusability of the Tergitol@SiO_2@Fe_3O_4 magnetic nano-material on the recovery of Pb(II) ions was investigated under optimized conditions. It has been observed from experimental studies that the Tergitol@SiO_2@Fe_3O_4 magnetic nano-material can be reused at least 12 times with a <5% loss in the recovery of Pb (II) ions. This result has shown that the Tergitol@SiO_2@Fe_3O_4 magnetic nano-material has great potential to be used repeatedly for the extraction and separation of Pb(II) ions.

3.5. Adsorbent capacity

Adsorbent capacity is defined as the maximum amount of analyte retained by a certain amount of sorbent. To evaluate the sorbent capacity of the Tergitol@SiO_2@Fe_3O_4 magnetic nano-material, 41.5 mg of the adsorbent was poured to 150 mL of the model solution containing Pb (II) ions (50 μg L^{-1}). The resulting mixture was stirred for 15 min to ensure adsorption. The aqueous part was separated by decantation and subsequently aspirated to FAAS for lead analysis. The adsorbent capacity of the Tergitol@SiO_2@Fe_3O_4 magnetic nano-material was calculated from the following equation.

$$Q_e = (C_i - C_e)V\ W^{-1} \quad (1)$$

where Qe was the adsorbent capacity (mg g^{-1}), Ci and Ce were the initial and final amounts (mg L^{-1}) of Pb(II) ions, W (g) was the amount of the Tergitol@SiO_2@Fe_3O_4 magnetic nano-material and V was the volume of the model solution. As a result of the studies, the adsorbent capacity was calculated as 82.1 mg g^{-1} showing that it has strong adsorption capability for the Pb(II).

Table 2a
Analytical data obtained as a result of applying the optimized method to two CRMs (95% confidence interval; t-critical: 2.13. N = 5).

CRMs	[a.b]Certified value	[a.b]Found	Recovery (%)	RSD (%)	t_{-exp}
INCT-TL-1-tea leaves	1.78 ± 0.24	1.74 ± 0.06	97.8	3.5	1.49
1643e Trace elements in water	19.63 ± 0.21	19.85 ± 0.41	101.1	2.1	1.20

[a] mg kg^{-1}; [b] μg L^{-1}.

3.6. Effect of sample volume

To calculate the preconcentration factor (PF), the sample volume needs to be determined because PF is defined as the ratio of the sample volume to the measurement volume. In this context, the effect of sample volume on the recovery of Pb(II) ions was investigated in the volume range of 10–200 mL under the optimized conditions. As a result of the studies carried out (see Fig. 3c), quantitative recovery has been obtained up to 150 mL sample volume. But, recovery was decreased after this volume. To ensure the high preconcentration factor, 150 mL sample volume was chosen as the optimum value.

3.7. Method performance

3.7.1. Analytical figures of merit

Analytical characteristics of the optimized method, i.e., calibration equation, linear range, limit of detection (LOD), limit of quantification (LOQ), adsorbent capacity, PF, and enhancement factor (EF) were investigated under the optimal conditions. The calibration curves were drawn using 15 concentration levels of standard Pb(II) ions and wide linear range were obtained from 0.2 to 250 μg L^{-1} with the correlation coefficient (r2:0.9992). The calibration equation obtained for this calibration curve was A = 0.0017 + 0.09825[Pb(II) μg L^{-1}]. The LOD based on three times standard deviation of ten replicates of sample blank absorbance divided by the slope of calibration curve after magnetic-SPME were calculated as 0.07 μg L^{-1}. The average recovery value of the magnetic-SPME method was 97.5%. The PF was calculated as 100 from the ratio of the initial sample volume (150 mL) to the measurement volume (1.5 mL). The EF was calculated as 84 from the ratio of the slopes of calibration curves before and after magnetic-SPME. Detailed data were given in Supplementary Material Table S2.

3.7.2. Inter-day and intra-day studies

To evaluate the accuracy and precision of the optimized method, relative standard deviation (RSD%) and recovery were referenced, respectively. In Inter-day studies were investigated for three different concentrations of Pb(II) in five replicates each on the same day. In the intra-day study were investigated for the same concentrations in five replicates each on three consecutive days. The Pb(II) concentrations used in this study were 5 μg L^{-1}, 50 μg L^{-1}, and 100 μg L^{-1}, respectively. From the inter-day studies, the RSD% and recovery were in the range 2.1–3.4% and 93.7–98.1%, respectively. In addition, for intra -day studies, the RSD% and recovery were ranged from 2.5 to 4.3% and 92.7–104.6%, respectively. All analytical results were within acceptable limits according to the validation guideline used [34].

3.7.3. Selectivity

The selectivity of the synthesized adsorbent for Pb(II) ions was investigated in the presence of coexisting ions. Each ions was added to the model solution including Pb(II), respectively, and the absorbance was compared with that corresponding to the solution absorbance containing only the Pb(II). An ion was considered to interfere when the absorbance in its presence varies ± 5% concerning the absorbance of Pb (II) ions. The tolerance limit was calculated from the ratio of the amount of ion causing this change to the amount of Pb(II) ions in the model solution. As can be seen from the results in Supplementary Material Table S3, low RSD and quantitative recovery and high tolerance limits were obtained for the studied ions. These results indicate that the synthesized magnetic adsorbent has high selectivity for Pb(II) ions.

Table 2b
Determination of Pb in water samples and analyte recovery study.

Samples	*Added	*Found	RSD (%)	Recovery (%)
Tap water	–	**n.d	1.7	–
	100	98.8 ± 1.8	1.8	98.8
Bottled water	–	n.d	1.5	–
	100	96.5 ± 1.6	1.7	96.5
River water	–	3.6 ± 0.08	2.2	–
	100	100.8 ± 2.4	2.4	97.2
Wellwater	–	7.1 ± 0.1	1.4	–
	100	110.5 ± 2.0	1.8	103.4

*μg L^{-1} ** could not be detected.

Table 2c
Determination of Pb in real samples and analyte recovery study.

Samples	*Added	*Found (Mean ± S.D, n = 3)	Recovery (%)
Meat doner-1	–	4.2 ± 0.3	–
	100	102.6 ± 1.8	98.4
Meat doner-2	–	6.7 ± 0.4	–
	100	97.9 ± 2.7	91.2
Chicken doner-1	–	11.9 ± 0.9	–
	100	108.6 ± 3.5	96.7
Chicken doner-2	–	3.3 ± 0.1	–
	100	106.2 ± 2.6	102.9
Meatballs-1	–	8.9 ± 1.0	–
	100	104.7 ± 3.7	95.8
Meatballs-2	–	18.7 ± 1.2	–
	100	111.8 ± 3.9	93.1
Grilled chicken-1	–	22.6 ± 1.3	–
	100	120.9 ± 3.2	98.3
Grilled chicken-2	–	7.1 ± 0.5	–
	100	103.6 ± 2.8	96.5
Fish	–	12.1 ± 0.9	–
	100	113.8 ± 2.4	101.7

*μg g^{-1}.

3.7.4. CRMs analysis

Prior to applying the optimized method to real samples, the validity of the method was examined by analysis of two CRMs (INCT-TL-1-tea leaves and 1643e Trace elements in water) containing lead. The amounts of lead found were 1.74 ± 0.06 mg kg^{-1} for INCT-TL-1-tea leaves and 19.85 ± 0.41 μg L^{-1} for 1643e Trace elements in water, respectively. The results found were very consistent with the reference values. Also, the statistical t-value for the 95% confidence level (N = 5, t-critical: 2.13) was greater than the experimental t-values for both CRMs. This ultimately confirms the accuracy of the method. Also, low RSD% and quantitative recoveries were obtained for CRMs. Detailed results were given in Table 2(a).

3.7.5. Application to real samples

Following optimization and validation studies, the optimized method was applied to the determination and preconcentration of lead in various water samples and foods. Analytical results for different water samples were given in Table 2(b). The recoveries and RSDs of water samples were in the range of 96.5–103.4% and 1.4–2.4% respectively. These results show the reliability of the method developed for the detection of lead in water samples. In addition, the magnetic-SPME method was applied after a level standard addition (μg g^{-1}) to food samples prepared by microwave digestion. As a result of the application, the highest lead (22.6 ± 1.3 μg g^{-1}) contents were detected in grilled chicken-1. Recovery values were in the range 91.2–102.9%. Comprehensive results were given in Table 2(c).

3.8. Comparison of the optimized method with other existing methods

To evaluate the contribution of the method to the literature, the comparison of the analytical value of the optimized method for preconcentration and determination of lead with some other available methods in the literature is given in Table 3. As shown from the results, the optimized method demonstrated its unique advantage over other methods, referring to high sorption capacity, low RSD, and low LOD. The linearity was superior or comparable to the reported methods. Also, the PF was better in most other methods, due to the high selectivity of the magnetic adsorbent synthesized for lead ions. Compared to other studies, the sample volume of the presented method is larger. This shows that there is no significant change in the analytical signal due to the dilution of the sample solution. Furthermore, the synthesis step of the magnetic adsorbent was simple and provided good reusability.

4. Conclusions

A simple, effective and economical magnetic-SPME method based on Tergitol@SiO_2@Fe_3O_4 nanoparticles as the adsorbent followed by FAAS determination was optimized by experimental modelling for the extraction and detection of Pb(II) ions from various water samples and foods. For this purpose, a 3-factor 3-level Box–Behnken design was applied to optimize the adsorption step. The optimal conditions were set as adsorbent amount of 41.5 mg, adsorption time 11.5 min, and pH 4.7. The magnetic adsorbent was highly selective for Pb(II) ions as there were no significant interference from coexisting ions even at high amounts. The low value of RSD indicated that the method was reproducible. Compared to other analytical procedures, the optimized

Table 3
Comparison of the published SPE procedure with the optimized method.

Sample matrix	Extraction procedure	Detection method	Linearity (μg L^{-1})	LOD (μg L^{-1})	RSD (%)	Recovery (%)	Adsorbent capacity (mg g^{-1})	PF	Sample volume (mL)	Refs.
Foods	AA-DES-LPME	GFAAS	0.12–2.5	0.006	2.9	97.0	–	60	60	[8]
Water and plant	Magnetic SPME	FAAS	100–1000	3.3	4.9	–	11.67	50	35	[35]
Water and foods	Magnetic SPME	FAAS	–	2.39	0.85	96	–	76	40	[36]
Waters	Magnetic SPME	GFAAS	0.025–2.0	0.00722	4.5	92.7	68.7	40	50	[37]
Sea water and mussel	DLLME	SQT-FAAS	–	2.7	4.45	–	–	141	8	[38]
Honey	UA-DLLME	FAAS	0.3–400	0.29	4.1	95.3	–	105	150	[39]
Vegetables	HI-DESME	FAAS	1–300	0.35	3.7	96.8	–	93	75	[40]
Water and foods	Magnetic SPME	FAAS	0.2–250	0.07	1.8	97.5	82.1	100	150	Optimized method

GFAAS: Graphite furnace atomic absorption spectrometry.
DLLME: Dispersive liquid–liquid microextraction.
SQT-FAAS: Slotted quartz tube coupled to flame atomic absorption spectrometry.
AA-DES-LPME: Air assisted liquid phase microextraction based on deep eutectic solvent.
UA-DLLME: Ultrasound assisted- dispersive liquid liquid micro.
HI-DESME: Heat-Induced Deep Eutectic Solvent Microextraction extraction.

method boasts a low LOD, wide linearity, high adsorbent capacity, good recovery, recyclable, and fastness. Consequently, the analytical data shown that the optimized method can be used as a green, simple and efficient extraction and detection techniques for trace lead in different matrixes.

CRediT authorship contribution statement

Nail Altunay: Supervision, Investigation, Validation, Writing - original draft, Writing - review & editing. **Adil Elik:** Investigation, Conceptualization, Validation. **Gökhan Sarp:** Investigation. **Erkan Yılmaz:** Conceptualization, Validation. **Halil İbrahim Ulusoy:** Investigation, Software, Writing - original draft.

Declaration of Competing Interest

The authors declare that they have no known competing financial interests or personal relationships that could have appeared to influence the work reported in this paper.

Appendix A. Supplementary data

Supplementary data to this article can be found online at https://doi.org/10.1016/j.microc.2021.106765.

References

[1] R. da Cruz Ferreira, F. de Souza Dias, C. de Aragão Tannus, F.B. Santana, D.C.M. B. dos Santos, F. de Souza Dias, M.S. de Castro, H.N. Brandão, A. de Freitas Santos Júnior, L.C.R. Cerqueira e Silva, F.A. Chinalia, Essential and potentially toxic elements from brazilian geopropolis produced by the stingless bee melipona quadrifasciata anthidioides using ICP OES, Biol. Trace Elem. Res. 199 (9) (2021) 3527–3539.

[2] R. Khanam, A. Kumar, A.K. Nayak, M. Shahid, R. Tripathi, S. Vijayakumar, D. Chatterjee, Metal (loid) s (As, Hg, Se, Pb and Cd) in paddy soil: bioavailability and potential risk to human health, Sci. Total Environ. 699 (2020), 134330.

[3] E. Skrzydlewska, M. Balcerzak, F. Vanhaecke, Determination of chromium, cadmium and lead in food-packaging materials by axial inductively coupled plasma time-of-flight mass spectrometry, Anal. Chim. Acta 479 (2) (2003) 191–202.

[4] L.H. Mason, J.P. Harp, D.Y. Han, Pb neurotoxicity: neuropsychological effects of lead toxicity, Biomed Res. Int. 2014 (2014) 1–8.

[5] K. Chibowska, I. Baranowska-Bosiacka, A. Falkowska, I. Gutowska, M. Goschorska, D. Chlubek, Effect of lead (Pb) on inflammatory processes in the brain, Int. J. Mol. Sci. 17 (12) (2016) 2140.

[6] M.D. Lakshmi Priya, A. Geetha, Level of trace elements (copper, zinc, magnesium and selenium) and toxic elements (lead and mercury) in the hair and nail of children with autism, Biol. Trace Elem. Res. 142 (2) (2011) 148–158.

[7] M. Salarian, A. Ghanbarpour, M. Behbahani, S. Bagheri, A. Bagheri, A metal-organic framework sustained by a nanosized Ag12 cuboctahedral node for solid-phase extraction of ultra traces of lead (II) ions, Microchim. Acta 181 (9-10) (2014) 999–1007.

[8] R.A. Zounr, M. Tuzen, M.Y. Khuhawar, A simple and green deep eutectic solvent based air assisted liquid phase microextraction for separation, preconcentration and determination of lead in water and food samples by graphite furnace atomic absorption spectrometry, J. Mol. Liq. 259 (2018) 220–226.

[9] M.G. Kakavandi, M. Behbahani, F. Omidi, G. Hesam, Application of ultrasonic assisted-dispersive solid phase extraction based on ion-imprinted polymer nanoparticles for preconcentration and trace determination of lead ions in food and water samples, Food Anal. Methods 10 (7) (2017) 2454–2466.

[10] S. Garcia, F. Gerondi, T.R. Paixão, M.A. Arruda, I. Gaubeur, Cadmium and lead determination in freshwater and hemodialysis solutions by thermospray flame furnace atomic absorption spectrometry following cloud point extraction, J. Braz. Chem. Soc. 26 (3) (2015) 490–497.

[11] D. Martínez, G. Grindlay, L. Gras, J. Mora, Determination of cadmium and lead in wine samples by means of dispersive liquid–liquid microextraction coupled to electrothermal atomic absorption spectrometry, J. Food Compos. Anal. 67 (2018) 178–183.

[12] M. Shirani, S. Habibollahi, A. Akbari, Centrifuge-less deep eutectic solvent based magnetic nanofluid-linked air-agitated liquid–liquid microextraction coupled with electrothermal atomic absorption spectrometry for simultaneous determination of cadmium, lead, copper, and arsenic in food samples and non-alcoholic beverages, Food Chem. 281 (2019) 304–311.

[13] T. Borahan, T. Unutkan, N.B. Turan, F. Turak, S. Bakırdere, Determination of lead in milk samples using vortex assisted deep eutectic solvent based liquid phase microextraction-slotted quartz tube-flame atomic absorption spectrometry system, Food Chem. 299 (2019), 125065.

[14] L. Yao, H. Liu, X. Wang, W. Xu, Y. Zhu, H. Wang, C. Lin, Ultrasound-assisted surfactant-enhanced emulsification microextraction using a magnetic ionic liquid coupled with micro-solid phase extraction for the determination of cadmium and lead in edible vegetable oils, Food Chem. 256 (2018) 212–218.

[15] L. Yao, X. Wang, H. Liu, C. Lin, L. Pang, J. Yang, Q. Zeng, Optimization of ultrasound-assisted magnetic retrieval-linked ionic liquid dispersive liquid–liquid microextraction for the determination of cadmium and lead in water samples by graphite furnace atomic absorption spectrometry, J. Ind. Eng. Chem. 56 (2017) 321–326.

[16] M. Ghorbani, S. Akbarzade, M. Aghamohammadhasan, O. Seyedin, N. Afshar Lahoori, Pre-concentration and determination of cadmium and lead ions in real water, soil and food samples using a simple and sensitive green solvent-based ultrasonic assisted dispersive liquid–liquid microextraction and graphite furnace atomic absorption spectrometry, Anal. Methods 10 (17) (2018) 2041–2047.

[17] E. Akkaya, F.A. Erulas, Ç. Büyükpinar, S. Bakirdere, Accurate and sensitive determination of lead in black tea samples using cobalt magnetic particles based dispersive solid-phase microextraction prior to slotted quartz tube-flame atomic absorption spectrometry, Food Chem. 297 (2019), 124947.

[18] H.İ. Ulusoy, Applications of magnetic nanoparticles for the selective extraction of trace species from a complex matrix, in: M. Locatelli, C. Celia (Eds.), Anal. Chem. Dev. Appl. Challenges Food Anal., (2017) 55–75.

[19] J. Płotka-Wasylka, N. Szczepańska, M. La Guardia, J. Namieśnik, Miniaturized solid-phase extraction techniques, TrAC, Trends Anal. Chem. 73 (2015) 19–38.

[20] K.M. Hamid, JAK-STAT Lodges in multiple sclerosis: pathophysiology and therapeutic approach overview, Open Access Library J. 4 (04) (2017) 1.

[21] H.İ. Ulusoy, E. Yılmaz, M. Soylak, Magnetic solid phase extraction of trace paracetamol and caffeine in synthetic urine and wastewater samples by a using core shell hybrid material consisting of graphene oxide/multiwalled carbon nanotube/Fe3O4/SiO2, Microchem. J. 145 (2019) 843–851.

[22] M. Eftekhari, M. Gheibi, M. Akrami, F. Iranzad, Solid-phase extraction of ultra-trace levels of lead using tannic acid-coated graphene oxide as an efficient adsorbent followed by electrothermal atomic absorption spectrometry; response surface methodology–central composite design, New J. Chem. 42 (2) (2018) 1159–1168.

[23] N. Altunay, R. Gürkan, A simple and efficient approach for preconcentration of some heavy metals in cosmetic products before their determinations by flame atomic absorption spectrometry, Turk. J. Chem. 40 (6) (2016) 988–1001.

[24] P. Baile, L. Vidal, M.Á. Aguirre, A. Canals, A modified ZSM-5 zeolite/Fe 2 O 3 composite as a sorbent for magnetic dispersive solid-phase microextraction of cadmium, mercury and lead from urine samples prior to inductively coupled plasma optical emission spectrometry, J. Anal. At. Spectrom. 33 (5) (2018) 856–866.

[25] Z. Ni, Z. Chen, J. Cheng, F. Tang, Simultaneous determination of arsenic and lead in vegetable oil by atomic fluorescence spectrometry after vortex-assisted extraction, Anal. Lett. 50 (13) (2017) 2129–2138.

[26] A.A. Krata, M. Wojciechowski, M. Kalabun, E. Bulska, Reference measurements of cadmium and lead contents in candidates for new environmental certified materials by isotope dilution inductively coupled plasma mass spectrometry, Microchem. J. 142 (2018) 36–42.

[27] H. Tinas, N. Ozbek, S. Akman, Determination of lead in flour samples directly by solid sampling high resolution continuum source graphite furnace atomic absorption spectrometry, Spectrochim. Acta, Part B 140 (2018) 73–75.

[28] X. Tan, Z. Wang, Z. Wang, A Facile Acidic Digestion Method for Cosmetic Lead and Cadmium Determination by an Inductively Coupled Plasma Atomic Emission Spectrometer, J. Appl. Spectrosc. 85 (4) (2018) 659–664.

[29] S.M. Sorouraddin, M.A. Farajzadeh, H. Dastoori, Development of a dispersive liquid-liquid microextraction method based on a ternary deep eutectic solvent as chelating agent and extraction solvent for preconcentration of heavy metals from milk samples, Talanta 208 (2020), 120485.

[30] N. Altunay, D. Bingöl, A. Elik, R. Gürkan, Vortex assisted-ionic liquid dispersive liquid-liquid microextraction and spectrophotometric determination of quercetin in tea, honey, fruit juice and wine samples after optimization based on response surface methodology, Spectrochim. Acta Part A Mol. Biomol. Spectrosc. 221 (2019) 117166, https://doi.org/10.1016/j.saa.2019.117166.

[31] P.K. Sahu, N.R. Ramisetti, T. Cecchi, S. Swain, C.S. Patro, J. Panda, An overview of experimental designs in HPLC method development and validation, J. Pharm. Biomed. Anal. 147 (2018) 590–611.

[32] S. Sahin, H.I. Ulusoy, S. Alemdar, S. Erdogan, S. Agaoglu, The presence of polycyclic aromatic hydrocarbons (PAHs) in grilled beef, chicken and fish by considering dietary exposure and risk assessment, Food Sci. Animal Resour. 40 (5) (2020) 675–688.

[33] T. Oymak, H.İ. Ulusoy, E. Hastaoglu, V. Yılmaz, Ş. Yıldırım, Some heavy metal contents of various slaughtered cattle tissues in Sivas-Turkey, J. Turkish Chem. Society Section A: Chem. 4 (3) (2017) 721–728.

[34] INMETRO. Instituto Nacional de Metrologia, Qualidade e Tecnologia. (2016). Orientação sobre validação de métodos analíticos.

[35] N. Baghban, E. Yilmaz, M. Soylak, A magnetic MoS 2-Fe 3 O 4 nanocomposite as an effective adsorbent for dispersive solid-phase microextraction of lead (II) and copper (II) prior to their determination by FAAS, Microchim. Acta 184 (10) (2017) 3969–3976.

[36] M. Khan, E. Yilmaz, B. Sevinc, E. Sahmetlioglu, J. Shah, M.R. Jan, M. Soylak, Preparation and characterization of magnetic allylamine modified graphene oxide-poly (vinyl acetate-co-divinylbenzene) nanocomposite for vortex assisted magnetic solid phase extraction of some metal ions, Talanta 146 (2016) 130–137.

[37] Y. Huang, J. Peng, X. Huang, Allylthiourea functionalized magnetic adsorbent for the extraction of cadmium, copper and lead ions prior to their determination by atomic absorption spectrometry, Microchim. Acta 186 (2) (2019) 51.

[38] S. Erarpat, G. Özzeybek, D.S. Chormey, S. Bakırdere, Determination of lead at trace levels in mussel and sea water samples using vortex assisted dispersive liquid-liquid microextraction-slotted quartz tube-flame atomic absorption spectrometry, Chemosphere 189 (2017) 180–185.
[39] N. Altunay, A. Elik, R. Gürkan, Monitoring of some trace metals in honeys by flame atomic absorption spectrometry after ultrasound assisted-dispersive liquid liquid microextraction using natural deep eutectic solvent, Microchem. J. 147 (2019) 49–59.
[40] N. Altunay, A. Elik, D. Bingöl, Simple and green heat-induced deep eutectic solvent microextraction for determination of lead and cadmium in vegetable samples by flame atomic absorption spectrometry: a multivariate study, Biol. Trace Elem. Res. 1–8 (2020).